

# 飽和된 砂質土 내로의 汚染物 이동에 관한 信賴性 : 遂行 및 檢證

## Reliability Analysis to Contaminant Migration in Saturated Sandy Soils : Implementation and Verification

張 演 洙  
Jang, Yeon Soo

### 요 지

본 논문에서는 一階 및 二階 信賴解析法을 이용 汚染物 이동의 해석할 수 있는 모델을 개발하였으며 오염이동 모델은 1차원 차분법과 2차원 유한요소법을 이용하였다. 一階 및 二階 신뢰성 해석법은 흙의 특성을 제한하는 가정사항이 필요치 않은 확률모델이며 본 해석으로부터 얻어지는 예민도 (sensitivity)는 확률해에 큰 영향을 미치는 입력 매개변수에 대한 정보를 제공한다.

1차원 오염물 이동 신뢰성 해석으로 신뢰성해석 프로그램의 유용성과 정밀성을 검증하였으며, 연속 오염원의 2차원 해석과 농도 극한상태 함수를 이용하여 오염물 이동 경로상 지점의 입력변수가 신뢰성해석의 확률해에 미치는 영향을 검토하였다.

### Abstract

The first and second-order reliability method(FORM and SORM) is presented using one dimensional finite difference and two dimensional finite element transport models. FORM and SORM can be used without any restrictive assumptions about the properties of the media, and the sensitivity information obtained as part of these analyses is used to identify the parameters which have major influence on the estimate of probability. The reliability analysis of transport in a one-dimensional domain is used to test the robustness of the reliability code and to evaluate the accuracy of the reliability method. A continuous source 2-D example with a concentration threshold limit state function is used to evaluate the influence of the parameters in the location of interest on the reliability solution.

### 1. Introduction

The problems caused by the migration of contaminants in groundwater have generated a great

deal of interest in developing predictive models to the scientist and engineers for the possible mechanisms. The analysis of contaminant transport in natural environment is complicated by the inherent heterogeneity of the materials and the traditional deterministic methods have difficulty

\* 정희원 · 한국건설기술연구원, 지반연구실 선임연구원

in adequately characterizing the transport process. The analysis of contaminant migration involves significant prediction uncertainty and, there is a need to develop probabilistic techniques for the analysis of contaminant transport.

The applications of these techniques to evaluation of the prediction uncertainty were explored in recent papers by Sitar et al.<sup>(1)</sup>, Cawfield and Sitar<sup>(2)</sup>, and Wagner and Gorelik.<sup>(3)</sup> Sitar et al.<sup>(1)</sup> have applied the first-order and second moment reliability method(FORM) to three ksubsurface flow and contaminant migration examples and illustrated the capability of the method. Cawfield and Sitar<sup>(2)</sup> extended this approach to a 2-D finite-element analysis of steady-state groundwater flow and investigated the effects of spatial variability. Input parameters used in their analysis are assumed to be random and the spatial variability of hydraulic conductivities was incorporated by defining in terms of correlated random variables at every element in the flow domain. The importance of the spatial variability of the hydraulic conductivity was shown in terms of its effect on computed reliability estimates. Wagner and Gorelik<sup>(3)</sup> used the first-order reliability approach coupled with a management model to find an optimal pumping strategy which satisfies the given water quality objectives. The mean centered first order reliability method was used to estimate the statistical moments of the random variables. Unknown parameters estimated were: the effective porosity, hydraulic conductivity, longitudinal and transverse dispersivity. The estimated parameter values were input into the optimization model. The uncertainty model in this analysis did not incorporate spatial variability.

In the present paper, the first and second order reliability methods, FORM and SORM, are introduced to the extent needed to understand their application to contaminant transport. A one-dimensional finite difference model of advection dominated transport is used to evaluate the robustness of the reliability algorithms and to evaluate their accuracy. Specifically, the influence of correlation length and input parameter variance is examined.

Example application of the first and second order reliability models to 2-D contaminant transport analysis are presented. The purpose of the 2-D transport reliability model is to extend the reliability analysis to a wider range of problems, to be able to account for the transverse spreading of the contaminant which may influence the advance of the plume, and to handle more complex problems such as geological and statistical anisotropy. In the 2-D contaminant transport, the source was assumed to be continuous and the probability that a given concentration will be exceeded at a point of interest and time is evaluated.

## 2. First and Second Order Reliability Methods

In the analysis of contaminant transport, "failure" may be defined as the occurrence of a concentration equal to or greater than a specified threshold, i.e. a regulatory standard, over a given period of time in a region of interest. The reliability problem is then formulated in terms of a limit state function, denoted as  $g(X)$ , where  $X$  is the vector of the random variables, and  $g(X) \leq 0$  denotes the region in which the threshold value is met or exceeded (i.e. failure occurs). The boundary between the region in which the concentration is not exceeded and the region in which the concentration is exceeded is given by  $g(X) = 0$  and is called the limit state surface. One possible formulation of the limit state function for a threshold concentration,  $C_t$ , is:

$$g(X) = C_t - C(x, y, t) \quad (1)$$

where  $C(x, y, t)$  is the concentration at a specified location  $(x, y)$  at time  $t$ .

The probability that the threshold value is exceeded, or  $p = P[C_t \leq C(x, y, t)]$  is obtained by integrating the joint pdf in the region where  $g(X) \leq 0$ , i.e.

$$p = P[g(X) \leq 0] = \int_{g(X) \leq 0} f_X(X) dx \quad (2)$$

in which  $f_X(X)$  is the joint pdf of  $X$  and the  $n$ -fold

integral is over the unsafe region. In practice, a direct numerical evaluation of the multifold integral is virtually impossible. Hence, FORM and SORM have been developed to approximately evaluate the integral.<sup>(4)</sup>

In FORM and SORM, the integral given in equation (2) is evaluated in standard normal space by transforming the basic random variables,  $X$ , into a set standard normal variates,  $U=U(X)$  having the pdf:

$$\phi_n(\mathbf{u}) = (2\pi)^{-n/2} \exp \left[ -\frac{1}{2} |U|^2 \right] \quad (3)$$

where  $n$  is the number of random variables. With this transformation, the probability intergral in equation (2) is written in the form.

$$p = \int_{G(\mathbf{u}) < 0} \phi_n(\mathbf{u}) d\mathbf{u} \quad (4)$$

where  $G(\mathbf{u}) = g(\mathbf{X}(\mathbf{u}))$  is the limit-state function in the transformed space.

The point on the limit state surface closest to the origin, known as the design point and denoted by  $\mathbf{u}^*$  in Fig. 1, has the highest likelihood among all failure points and the region in the immediate neighbourhood of the design point is the main contributor to the probability intergral (equation 2). Thus, a good approximation of the probability integral can be obtained if the integration boundary in the standard normal space,  $G(\mathbf{U})=0$ , is replaced with an approximating surface which

closely matches the actual boundary in the neighborhood of the design point. This is the basic idea behind FORM and SORM.

In FORM, the limit state surface is replaced by a tangent hyperplane at the design point  $\mathbf{u}^*$ . The distance from the origin,  $\beta$ , known as the reliability index is given by the inner product

$$\beta = \alpha^* \mathbf{u}^* \quad (5)$$

where  $\alpha^*$  is the unit normal at the design point directed toward the failure region. The first order approximation,  $P_1$ , to  $P$  is

$$P_1 = \Phi(-\beta) \quad (6)$$

where  $\Phi(\cdot)$  is the standard cumulative normal probability.

The FORM approximation works well as long as the limit state surface has only one minimal distance point and is nearly flat in the neighbourhood of the design point. However, when the limit-state surface is curved, which may occur if the limit-state function is highly non-linear or when the input variables are strongly non-normal, a higher order approximation may be required. In the analysis of contaminant transport, especially if the simulated flow domain is a random field, such an approximation is typically necessary, because of the non-linearity of the limit-state function.

Point-fitting SORM, where the limit-state function is fitted with a piecewise paraboloid surface that is tangent at the design point is used to compute the probability of second order reliability.<sup>(5)</sup>

### 3. Sensitivity Measures

An important aspect of the first-order reliability method is that measures of sensitivity of the reliability index,  $\beta$ , and of the first-order estimate of the failure probability,  $P_1$ , with respect to the parameter defining the probability distribution and the limit state function are obtained as a part of the solution. The basic measure of sensitivity is the partial derivative of  $\beta$  with respect to the coordinates of the design point in the standard normal space given by

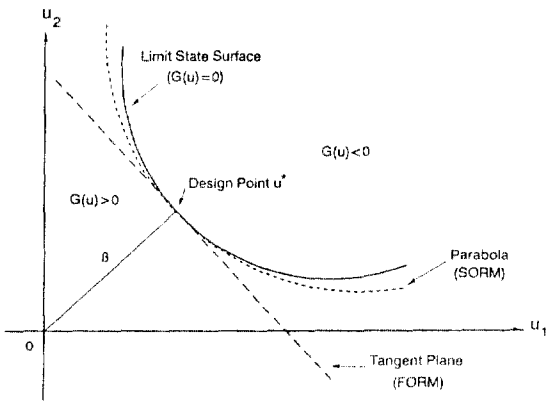


Fig. 1. First and second order approximation of limit state surface in standard space.

$$\nabla_{\mathbf{x}^*} \beta = \alpha^* \quad (7)$$

in which  $\alpha^* = -\nabla G(\mathbf{u}^*) / |\nabla G(\mathbf{u}^*)|$  is the vector normal to the limit-state surface at the design point and directed towards the failure set. The sensitivity of  $\beta$  with respect to the coordinates of the design point in the original space is given by the chain rule:

$$\nabla_{\mathbf{x}^*} \beta = \alpha^* \mathbf{J}_{\mathbf{u}^*, \mathbf{y}^*} \quad (8)$$

Since the values of  $\nabla_{\mathbf{x}^*} \beta$  are dependent on the units of  $\mathbf{x}$ , Der Kiureghian and Ke<sup>(6)</sup> scaled the gradient vector by the matrix of standard deviations and defined the unit vector

$$\gamma(\mathbf{x}) = \frac{\alpha(\mathbf{u})^T \mathbf{J}_{\mathbf{u}, \mathbf{x}} \mathbf{D}}{|\alpha(\mathbf{u})^T \mathbf{J}_{\mathbf{u}, \mathbf{x}} \mathbf{D}|} \quad (9)$$

where  $\mathbf{D}$  is the diagonal matrix of standard deviations of  $\mathbf{X}$ . Thus, the unit vector  $\gamma(\mathbf{x}^*)$  at the design point measures the scaled and normalized sensitivities of  $\beta$  with respect to the variations in the coordinates of  $\mathbf{x}^*$ . As such, this vector provides a measure of relative importance of each basic variable  $X_i$ .

The sensitivity of  $\beta$  with respect to parameters  $\theta$  defining the distribution function of  $\mathbf{x}$ , i.e.,  $f_i(\mathbf{x}, \theta)$  (such as means, standard deviations, etc.) is given by

$$\nabla \beta = \alpha^* \frac{\partial \mathbf{u}^*(\mathbf{x}^*, \theta)}{\partial \theta} \quad (10)$$

in which,  $\frac{\partial \mathbf{u}^*(\mathbf{x}^*, \theta)}{\partial \theta}$  represents the derivative of the random variables in the transformed space with respect to  $\theta$  at the design point.

#### 4. Transport Model Formulation

The analyses performed in this study are limited to transport of a conservative solute in a porous medium in a steady state flow which can be described by the advection equation of the form:

$$\frac{\partial C}{\partial t} + \bar{\mathbf{v}} \nabla C - \nabla \cdot (\mathbf{D} \cdot \nabla C) - C_s = 0 \quad (11)$$

where  $C$  is concentration of solute,  $C_s$  is concentration at the source nodes,  $\mathbf{D}$  is the dispersion coefficient, and  $\bar{\mathbf{v}}$  is the average linear velocity of groundwater. The dispersion coefficient in equation (11) is given by:

$$D_{xx} = \alpha_L \frac{\bar{v}_x^2}{|\bar{\mathbf{v}}|} + \alpha_T \frac{\bar{v}_y^2}{|\bar{\mathbf{v}}|} + D^* \quad (12a)$$

$$D_{yy} = \alpha_L \frac{\bar{v}_y^2}{|\bar{\mathbf{v}}|} + \alpha_T \frac{\bar{v}_x^2}{|\bar{\mathbf{v}}|} + D^* \quad (12b)$$

$$D_{xy} = D_{yx} = (\alpha_L - \alpha_T) \frac{\bar{v}_x \bar{v}_y}{|\bar{\mathbf{v}}|} \quad (12c)$$

where  $\alpha_L$  and  $\alpha_T$  are the longitudinal and transverse dispersivities.

The average linear flow velocity,  $\bar{\mathbf{v}}$ , is obtained from Darcy's law

$$\bar{\mathbf{v}} = -\frac{K}{n} \nabla h \quad (13)$$

where  $K$  and  $n$  denote element hydraulic conductivity and porosity, respectively. Two different numerical models are used to solve the advection-dispersion equation: a 1-D finite difference model and a 2-D Galerkin finite element model. The finite difference model employs a simple central difference approximation and is used to test the FORM and SORM algorithms and to perform sensitivity and verification analysis.<sup>(7)</sup>

The 2-D Galerkin finite element model uses a four isoparametric quadrilateral elements for spatial discretization for both flow and transport, and implicit finite difference approximation in time. This is a well known formulation (see e.g., Huyakorn and Pinder<sup>(8)</sup>) which produces two sets of linear algebraic equations as follows:

$$\begin{aligned} \sum_{e=1}^{nn} \left[ \int_A [\bar{\mathbf{v}} \nabla N_j N_i + \mathbf{D} \nabla N_j \nabla N_i + \frac{N_i}{\Delta t}] C_j^{m+1} dA \right] \\ = \sum_{e=1}^{nn} \left[ \int_A \frac{N_i}{\Delta t} C_j^m dA \right] \end{aligned} \quad (14a)$$

$$\sum_{e=1}^{nn} \left[ \int_A [K \nabla N_j \nabla N_i] h_j dA \right] = \sum_{e=1}^{nn} \left[ \int_A q_e N_i dA \right] \quad (14b)$$

where  $C_j^{m+1}$  is the concentration at node  $j$  at the time step  $(m+1)$ ,  $h_j$  is the hydraulic head at node  $j$ ,  $q_e$  is uniformly distributed flux,  $nn$  is the num-

ber of elements, and  $n$  is the number of nodal points.

The velocities in the numerical solution of the flow equation are computed at the Gaussian quadrature points in each element. For the contaminant transport solution, the velocity at a centroid is calculated by taking average of four global  $x$  and  $y$  components of velocity at the Gauss points, respectively. The reliability analysis are performed by coupling the respective transport modules to a reliability shell, CALREL.<sup>(9)</sup>

### 5. Reliability Analysis of Transport in a One-Dimensional Domain

FORM and SORM analyses of contaminant transport in a one-dimensional domain are used to demonstrate the robustness of the reliability code and to evaluate the accuracy of the reliability analysis methods. The problem posed is to estimate the probability that the concentration at a point located 40 m downgradient from a transient source lasting 30 days will exceed a specified concentration, within 300 days after the start of the injection. The discretized model has 81 nodes with 1.0 m spacing and a time step of 1 day is used. The source is located at  $x=10$  m and the observation point at  $x=50$  m. The dispersivity and hydraulic conductivity of the porous medium are characterized by those of sandy soils, i.e., by the means and standard deviations  $\mu_\alpha=1$  m,  $\sigma_\alpha=0.1$  m,  $\mu_K=3$  m/day,  $\sigma_K=0.3$  m/day, respectively. The distribution of  $K$  is assumed to be lognormal and the distribution of the other variables, i.e., dispersivity, boundary head, are assumed to be normal. All variables are assumed to be mutually, statistically independent. Porosity of the soil is assumed to be deterministic constant with a value of 0.3.

In order to examine the influence of spatial variability and to examine the influence of correlation length,  $K$  and  $\alpha$  are treated as random fields. Exponential correlation function,  $\rho(d)$  is used for the random field representation of  $K$  and  $\alpha$ , i.e.:

$$\rho(d) = \exp\left[-\frac{|d|}{\lambda}\right] \quad (15)$$

in which  $|d|$  denotes the distance between two points of interest and  $\lambda$  is the correlation length. Correlation length  $\lambda=2$  m and 10 m is used for most examples presented here.

The limit state function in this case is given by:

$$g(X) = a - C(50, 300) \quad a=0.05, 0.1, 0.2 \quad C_0 \quad (16)$$

in which  $C(50, 300)$  denotes the concentration which can be reached during the time interval of 300 days at  $x=50$  m. Negligible variation in hydraulic heads at the two boundaries and the concentration at the source is assumed because the influence of spatial variability in hydraulic conductivity and dispersivity is of main interest in these analyses. The mean hydraulic gradient across the domain, based on the mean values of the hydraulic heads at boundaries, is 0.01.

Fig. 2 shows the computed concentration profiles using FORM at the design point for threshold values of  $a=0.05, 0.1$  and  $0.2 \quad C_0$ , as compared with the concentration profile computed using the mean values of parameters which gives  $C=0.081 \quad C_0$  at  $x=50$  m. As already discussed, the values of the random variables at the design point give a solution with the highest probability of exceeding the specified threshold. The plotted design point concentration profiles obtained using the values of  $0.1 \quad C_0$  and  $0.2 \quad C_0$  are greater than the mean value solution at the point of interest.

The first-order estimate of the probability of

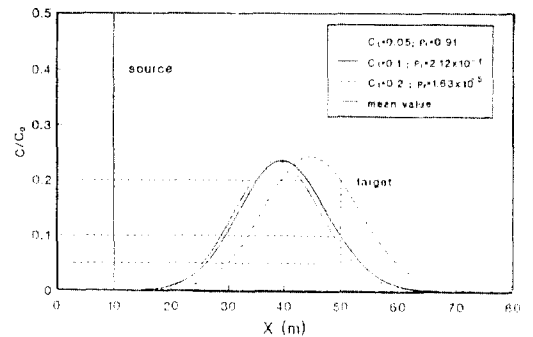


Fig. 2. Concentration distribution at the design point for the different threshold concentrations.

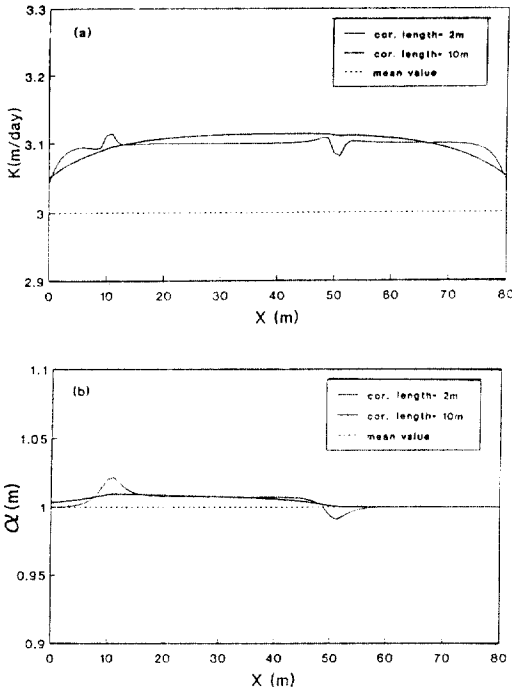


Fig. 3. Distribution of hydraulic conductivity (a), and dispersivity (b), at the design point for correlation length,  $\lambda_K = \lambda_\alpha = 2$  and 10m.

exceeding  $0.1 C_o$ ,  $P_1[C(50, 300) \geq 0.05 C_o]$  in which threshold concentration is smaller than mean value solution, has the value of 0.907. Thus, it is relatively unlikely that the concentration at the point of interest would reach the value  $0.2 C_o$ , 300 days after the start of contaminant release, and it is highly likely that the concentration at the target point would exceed the concentration  $0.05 C_o$ .

The hydraulic conductivity values at the design point corresponding to  $a=0.1 C_o$  and the sensitivity of this solution to  $K$  and  $\alpha$  are shown in Fig. 3 to 4. As can be seen in Fig. 3, the hydraulic conductivity at the design point is greater than the mean throughout the flow region while the dispersivity is greater than the mean upgradient from the point of interest.

These results are consistent with the requirement that for a given head gradient, higher  $K$  and  $\alpha$  values are needed to produce concentration

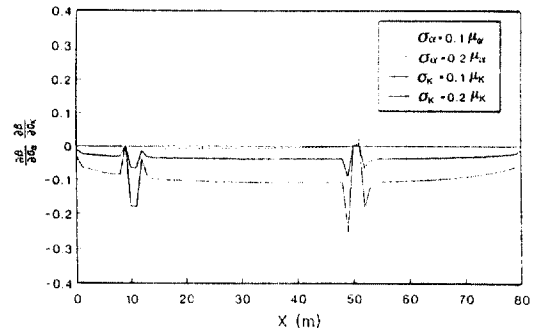


Fig. 4. Local Sensitivity of  $\beta$  to distribution parameters  $\sigma_K$  and  $\sigma_\alpha$ ;  $\lambda_K = \lambda_\alpha = 10m$

higher than the mean at the point of interest. Increasing the correlation length from 2m to 10m has relatively small effect, although the fluctuation in the design point values of  $K$  and  $\alpha$  are smoothed out as the correlation length increases, i.e., the domain becomes more uniform. The sensitivity of  $\beta$  to standard deviation of hydraulic conductivity and dispersivity is shown in Fig. 4. The sensitivities of  $\beta$  to  $\sigma$  of hydraulic conductivity are uniform over the domain except the node of interest and the source nodes. Negative sensitivity of  $\beta$  along the contaminant travel path indicates that  $\beta$  decreases if the standard deviation of input parameters along the travel path increases. Sensitivities decrease with increasing standard deviation for hydraulic conductivity.

The accuracy of the FORM and SORM analysis is evaluated by comparison with Monte Carlo simulations, since neither numerical nor analytical estimates of the probabilities of exceeding threshold values are available from previous stochastic analysis of contaminant transport.

The results of analyses for the two threshold values,  $C_t = 0.1$  and  $0.2 C_o$ , are plotted versus coefficient of variation of  $K$  in Fig. 5a, b. They show that for standard deviation  $\sigma_K < 0.1 \mu_K$  all three methods give comparable results; however, as the standard deviation increases above  $0.1 \mu_K$ , the first order reliability results diverge from the SORM and Monte Carlo results and tend to overestimate the probability of exceeding threshold values. The difference between FORM and SORM is due to

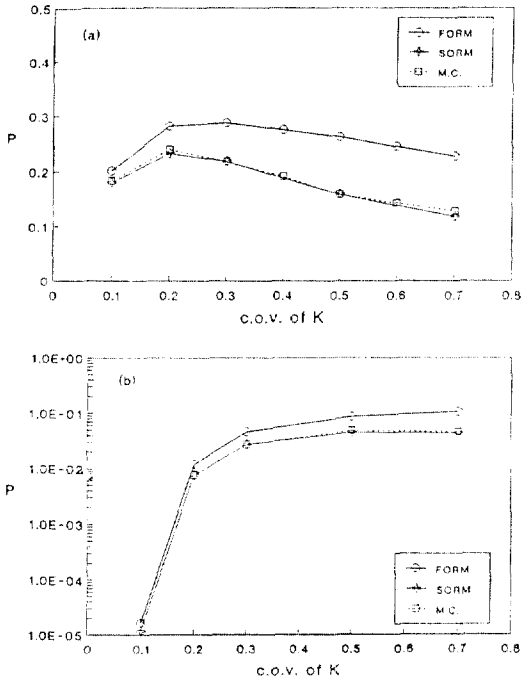


Fig. 5.  $P$  versus c.o.v. of  $K$  in a heterogeneous domain: (a) threshold concentration  $= 0.1C_0$  and (b) threshold concentration  $= 0.2C_0$ .

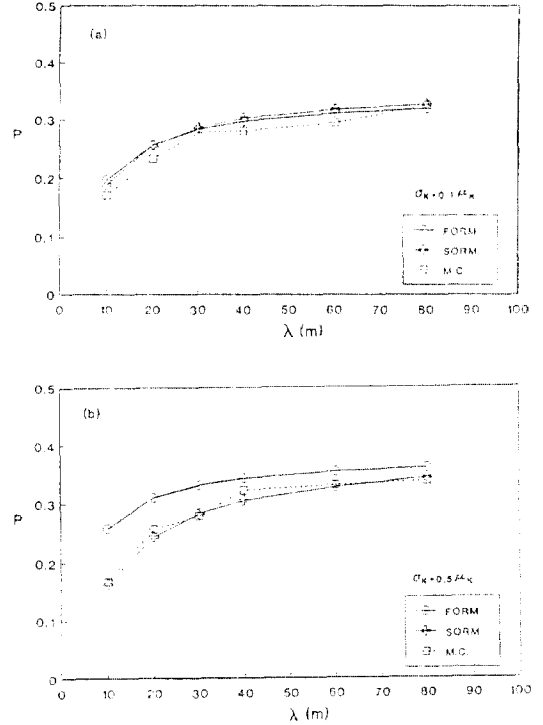


Fig. 6.  $P$  versus correlation length,  $\lambda_K$  and  $\lambda_{\sigma}$ , for (a) c.o.v. of  $k=0.1$  and (b) c.o.v. of  $K=0.5$

the fact that FORM neglects the curvature of the limit state surface at the design point which increases as  $\sigma_K$  increases.

The influence of correlation length on the computed probability assuming  $\sigma_K = 0.1\mu_K$  and  $\sigma_K = 0.5\mu_K$  is shown in Fig. 6a, b. In both cases the probability increases as the correlation length increases. This means that the plume may migrate faster as the hydraulic conductivities become more correlated, i.e., the medium is more homogeneous. For small  $\sigma_K$  the results of FORM and Monte Carlo simulation are fairly comparable (Fig. 6a); however, for large  $\sigma_K$  the discrepancy between the two results is significant, although the results tend to converge as the correlation length increases (Fig. 6b).

## 6. Reliability Analysis of Transport in a Two-dimensional Domain

The reliability analysis to two dimensional con-

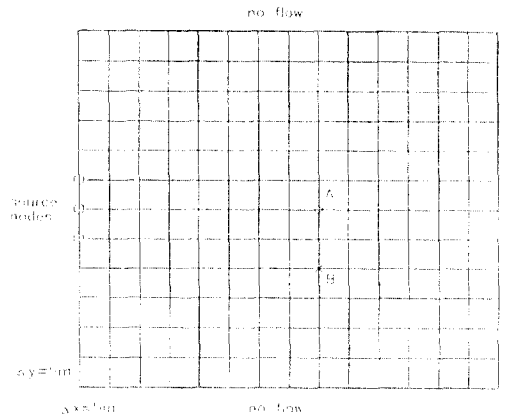


Fig. 7. Finite element mesh for concentration threshold analysis in a two-dimensional domain

taminant transport is presented to evaluate the probability of exceeding a threshold concentration in a steady state confined flow field with a continuous contaminant source. Fig. 7 shows the dis-

cretized domain measuring  $60 \times 70$  m and overlain by a grid consisting of 195 nodes and 168 quadrilateral elements.

Three continuous source nodes are located at the upstream boundary and two points of interest are considered: point A at location (40, 30) which is on the line of the maximum concentration and point B at location (40, 20) which is slightly off the line of the maximum concentration. The posed problem is to estimate the probability that the concentration at the node of interest exceeds concentration  $0.1 C_0$  during the course of 100 days of contaminant leakage which leads to the following limit state functions:

$$g(X) = 0.2 C_0 - C(40, 30, 100) \quad (17a)$$

$$g(X) = 0.2 C_0 - C(40, 20, 100) \quad (17b)$$

in which  $C(40, 30, 100)$  is the concentration at point A,  $C(40, 20, 100)$  is the concentration at point B, and the period of interest is 100 days.

The properties of the soil are assumed to have the following characteristics:  $\mu_K = 3\text{m/day}$ ,  $\sigma_K = 0.3\text{m/day}$ ;  $\mu_{\alpha_L} = 10\text{m}$ ,  $\sigma_{\alpha_L} = 1\text{m}$ ; and  $\mu_{\alpha_T} = 3\text{m}$ ,  $\sigma_{\alpha_T} = 0.3\text{m}$ . The distribution of the element hydraulic conductivities is assumed to be lognormal and all of the other variables are assumed to be normally distributed. Correlation length of spatially distributed variables  $K$ ,  $\alpha_L$  and  $\alpha_T$  is assumed 20m and the exponential correlation function is used. Hydraulic heads at the upstream and at the downstream boundary are modelled as random variables with  $\mu_h = 2.0\text{m}$ , and  $\mu_b = 0.6\text{m}$ , respectively, and  $\sigma_h = 0.14\text{m}$ . Porosity is assumed to be a deterministic constant with a value of 0.3. Thus, the total number of random variables in the problem with dispersivity modelled as a random field is 530, which includes three random variables  $K$ ,  $\alpha_L$  and  $\alpha_T$  in each element, and 26 constant boundary heads.

## 7. Analysis Results

The contours of concentration at the design point for both cases are shown in Fig. 8. The results show that shape of the contours of the con-

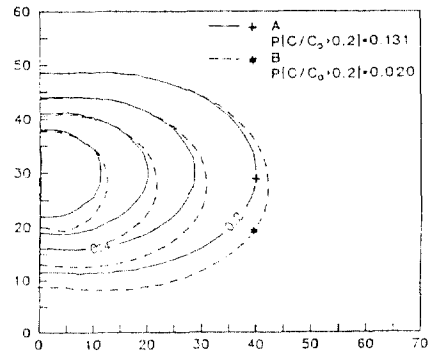


Fig. 8. Design point concentrations for cases A and B

centration at the design point for case B is shifted in the direction of the node of interest to give the required concentration  $0.2 C_0$  at the node.

The probability that the threshold concentration will be exceeded is greater in case A than in case B, as could be expected intuitively, given the position of the node of interest relative to the mean direction of travel of the contaminant plume.

The contours of  $K$  at the design point, i.e. the point which gives the highest probability of exceeding the threshold, are shown in Fig. 9 for both points of interest. In case A, the design point value of hydraulic conductivity is generally higher than  $\mu_K$  throughout the domain and gradually increase to a maximum along the center of the contaminant travel path (Fig. 9). Higher design point values of  $K$  result in higher flow velocity and the threshold concentration greater than the mean concentration at the node of interest can be reached. In case B, high design point values of  $K$  occur along a line connecting the source nodes and the node of interest.

The design point values of  $K$  in case B are generally higher than those in case A, since the threshold value is farther from the mean value solution and, therefore, higher  $K$  is needed to reach the threshold concentration.

Contour of local gamma sensitivity to  $K$  is shown in Fig. 10 for both cases. As would be expected, the gamma sensitivities to  $K$  are high at the source, the node of interest, and along the contaminant travel path between the source and



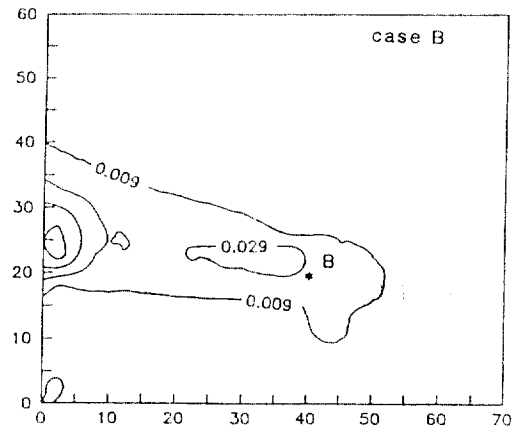
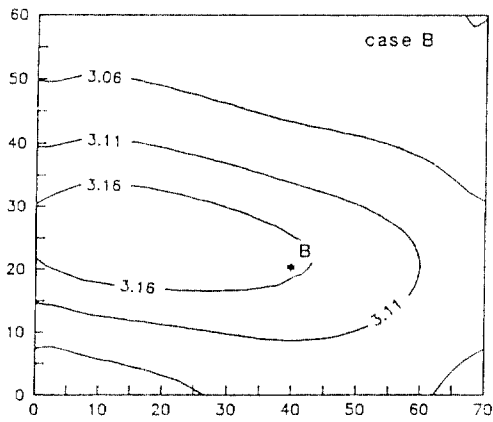
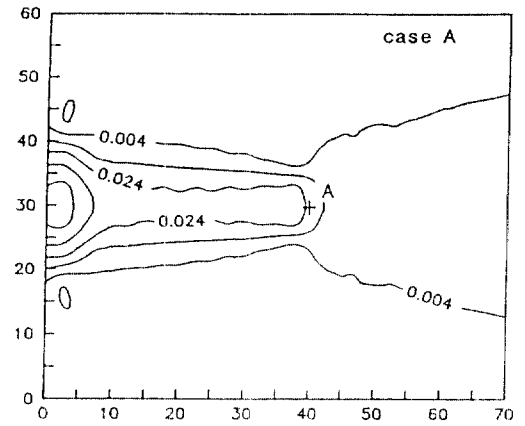
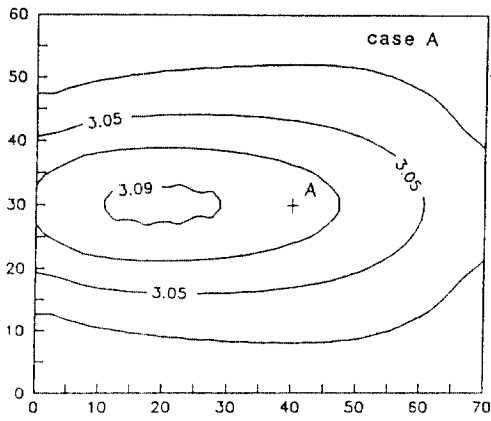


Fig. 9. Contours of hydraulic conductivity at the design point

Fig. 10. Contours of local gamma sensitivity to K

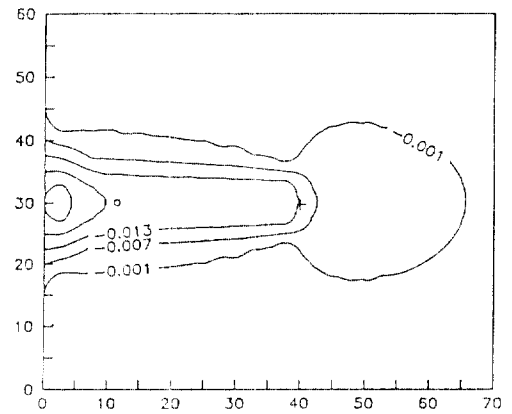
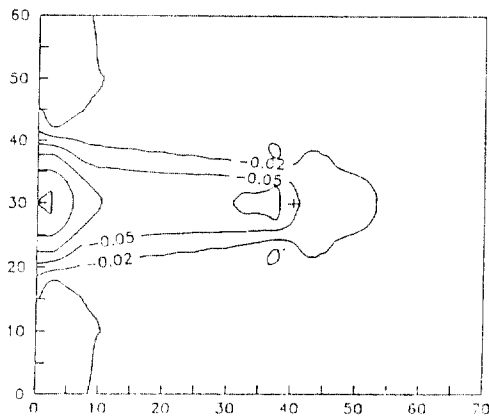


Fig. 11. Contours of local sensitivity of  $\beta$  to  $\mu_k$ ; case A

Fig. 12. Contours of local sensitivity of  $\beta$  to  $\sigma_k$ ; case A

the node of interest. Sensitivities are highest along the mean contaminant travel path in case A, and along the line connecting the source and the node of interest in case B.

An interesting result of the reliability analysis is the sensitivity of the reliability index,  $\beta$ , to the parameters of the distributions. Contour of local sensitivity of  $\beta$  to  $\mu_K$  is shown in Fig. 11.

The sensitivity of  $\beta$  to  $\mu_K$  is high along the contaminant travel path and it is highest at the source node and upgradient from the node of interest. Negative sensitivity values along the contaminant travel path indicate that  $\beta$  decreases as  $\mu_K$  increases. Sensitivity of  $\beta$  to  $\sigma_K$  are presented in Fig. 12. High negative sensitivities occur along contaminant travel path for both distribution parameters. Again in this case, negative sensitivity indicates that an increase in  $\sigma_K$  along the contaminant travel path reduces  $\beta$  and, therefore, probability of exceeding threshold increases.

## 8. Conclusion

Modeling contaminant transport in a subsurface environment is a difficult process because the parameters obtained in the field vary spatially and the governing scale of heterogeneity depends on the scale of the transport process. Advection-dispersion equation has been used most frequently for analysis of contaminant transport both in the laboratory and in the field. The problem with application of this equation to the field scale transport is that the uncertainties in the material properties and transport process cannot be accounted for explicitly.

In this paper, the application of the first and second order reliability of contaminant migration is presented, by linking the first and second order formulations to one dimensional numerical and two dimensional numerical transport routines. The 1-D transport reliability analysis was used to explore the influence of spatial variability and spatial correlation on the predicted probabilities of exceeding threshold concentrations. The results of the numerical analysis show that the  $P_f$  increa-

ses as correlation length increases. The computed sensitivities of the solution to the input parameter show that the solution is most sensitive to hydraulic conductivity at the source and the node of interest. Sensitivity distribution reflects the 1-D geometry of the domain in which a perturbation at any node can equally influence on the node of interest. In the case when the variance of the hydraulic conductivity is large, the first order reliability lacks sufficient accuracy and, for good accuracy, the second order reliability analysis need to be employed.

For the reliability analysis of the two-dimensional contaminant transport, concentration threshold limit state function was used to evaluate the influence of the position of the node of interest on the reliability solution. In the case when the node of interest is located along the axis of the maximum concentration of the plume, sensitivities to hydraulic conductivity and dispersivity are high along the contaminant travel path and they are highest around the source and the node of interest. In the case when the node of interest is located off the line of the maximum concentration, high sensitivities are located along the line connecting the source and the node of interest which is not necessarily the path of the center of the plume.

## References

1. Sitar, N., Cawfield J.D., and Kiureghian A., First Order Reliability Approach to Stochastic Analysis of Subsurface Flow and Contaminant Transport, *Water Resour. Res.*, 23(5), 794-804, 1987.
2. Cawfield, J.D., and N. Sitar, *Application of First-Order Reliability to Stochastic Finite Element Analysis of Groundwater Flow*, Report No. UCB/GT/87-01, June, 1987, 185 p.
3. Wagner, B.J., and S.M. Gorelik, Optimal Ground Water Management Under Parameter Uncertainty, *Water Resour. Res.*, 23(7), 1162-1174, 1987.
4. Madsen, H.O., S. Krenk, and N.C. Lind, *Methods of Structural Safety*, Prentice Hall, Inc., Englewood Cliffs, N.J., 1986.
5. Der Kiureghian, H-Z. Lin, and S-J. Hwang,

- Second Order Reliability Approximations, *J. Eng. Mech. Am. Soc. Civ. Eng.*, 113(8), 1208-1225, 1987.
6. Der Kiureghian, A., and J-B., Ke, Finite Element Based Reliability Analysis of Frame Structures, in *Proceedings, Fourth International Conference on Structural Safety and Reliability*, Vol. 1, 395-404, Kobe, Japan, May, 1985.
  7. Jang, Y.S., N.Sitar, and A. Der Kiureghian, *Reliability Approach to Probabilistic Modeling of Contaminant Transport*, Report No. UCB/GT-90/03, Dept. of Civil Eng., Univ. of Cal., Berkeley, July, 1990.
  8. Huyakorn, P.S., and G.F. Pinder, *Computational Methods in Subsurface Flow*, Academic Press, New York, 1983.
  9. Liu, P-L., H-Z. Lin and A. Der Kiureghian, *CAL-REL User's Manual*, Report No. UCB/SEMM-90/18, Dept. of Civil Eng., Univ. of Cal., Berkeley, Aug., 1989.

(接受：1992. 3. 2)